SIAM J. OPTIM.
Vol. 20, No. 4, pp. 1786–1810

OPTIMIZATION STRATEGIES FOR THE VULNERABILITY ANALYSIS OF THE ELECTRIC POWER GRID*

ALI PINAR†, JUAN MEZA‡, VAIBHAV DONDE§, AND BERNARD LESIEUTRE¶

Abstract. Identifying small groups of lines, whose removal would cause a severe blackout, is critical for the secure operation of the electric power grid. We show how power grid vulnerability analysis can be studied as a bilevel mixed integer nonlinear programming problem. Our analysis reveals a special structure in the formulation that can be exploited to avoid nonlinearity and approximate the original problem as a pure combinatorial problem. The key new observation behind our analysis is the correspondence between the Jacobian matrix (a representation of the feasibility boundary of the equations that describe the flow of power in the network) and the Laplacian matrix in spectral graph theory (a representation of the graph of the power grid). The reduced combinatorial problem is known as the network inhibition problem, for which we present a mixed integer linear programming formulation. Our experiments on benchmark power grids show that the reduced combinatorial model provides an accurate approximation, to enable vulnerability analyses of real-sized problems with more than 16,520 power lines.

Key words. mixed integer nonlinear programming, network inhibition, network flow, mixed integer linear programming, electric power flow, network vulnerability, graph theory

AMS subject classifications. 90C11, 90C27, 90C90, 90C30

DOI. 10.1137/070708275

1. Introduction.

Robust operation of a power grid requires anticipation of component outages that could lead to catastrophic blackouts. The current practice is to check for single contingencies to ensure the system stays intact after a single line outage. However, a small number of line outages (e.g., 3–5) can cause catastrophic blackouts, as evidenced by the Northeast Blackout in August 2003. In this article, we consider the *power network vulnerability analysis problem*, which aims to find small groups of lines whose loss can cause a severe blackout. Specifically, we pose the problem of computing the minimum number of line failures that will cause damage of at least a specified severity.

We consider the problem in a static sense by examining the relation between the operating point, which describes the current generation and consumption at each node in the network, and the feasibility boundary of the power flow equations. The severity of the events we identify could be different when dynamics and cascading events are considered. Our main focus here, therefore, is to identify simple events that can trigger a severe blackout, not to analyze its consequences, which requires

*Received by the editors November 15, 2009; accepted for publication (in revised form) November 27, 2009; published electronically February 5, 2010. This work was supported by the Director, Office of Science, Division of Mathematical, Information, and Computational Sciences of U.S. Department of Energy under contract DE-AC03-76SF00098.

http://www.siam.org/journals/siopt/20-4/70827.html

†Corresponding author. Information and Decision Sciences Department, Sandia National Laboratories, Livermore, CA 94550 (apinar@sandia.gov). The work was mostly performed when the author was with Lawrence Berkeley National Laboratory.

‡High Performance Computing Research Department, Lawrence Berkeley National Laboratory, Berkeley, CA 94720 (JCMeza@lbl.gov).

§Corporate research center, ABB Inc., Raleigh, NC 27606 (vaibhav.d.donde@us.abb.com). This work was performed at Lawrence Berkeley National Laboratory.

¶Environmental Energy Technologies Division, Lawrence Berkeley National Laboratory and Electrical and Computer Engineering Department, University of Wisconsin, Madison, WI 53706 (BCLesieutre@lbl.gov).

solving differential algebraic equations with discrete variables. Cascading events start with a significant disturbance that forces system elements to operate beyond their capabilities. For this reason, we look for minimal changes in the network topology that push the current operating point significantly outside of the feasibility region determined by the power flow equations.

This problem statement leads to a bilevel optimization problem since we are looking for minimal changes in network topology that maximize the distance between the current operating point and the new feasibility region. In this article, we present a bilevel mixed integer nonlinear programming (MINLP) formulation for the power network vulnerability analysis problem. The outer level seeks a minimal change in the topology and uses binary variables to specify lines to remove. The inner level implements a load shedding mechanism and computes the distance of the operating point to a new feasibility boundary, as a measure of the severity of the disturbance to the system. For this purpose, we solve a nonlinear optimization problem that optimally decreases the generation and consumption in the system to restore feasibility. We analyze the optimality conditions for the load shedding problem, present the Karush–Kuhn–Tucker (KKT) conditions for optimality, study the structure of the power flow Jacobian, and describe an augmented system for which we prove that Mangasarian–Fromovitz constraint qualification (MFCQ) conditions are satisfied. We use these results to present a single-level MINLP formulation of the vulnerability analysis problem that avoids solving nested optimization problems by replacing the inner optimization problem that computes the distance between the current operating point and the new feasibility region, with its corresponding KKT conditions.

A more detailed analysis of the structure of a feasible solution to our bilevel MINLP formulation reveals a special structure that can be exploited to reduce the problem to a pure combinatorial problem. We show that at a feasible solution to our bilevel MINLP formulation, the power network will be divided into two groups: one with excess generation and one with excess load, and the optimal load shedding strategy requires that in the load-rich region, we decrease only the consumption and keep the generation as is. Similarly in the generation-rich region, we decrease only the generation and keep the consumption as is. Moreover, we prove that at least one line that connects these two regions works at its maximum capacity to transfer power from the generation-rich side to the other side. This combinatorial structure of a feasible solution means that an optimal solution seeks a decomposition with maximum load/generation mismatch and minimum transmission capability between the two regions. This observation leads to our major result: the original bilevel MINLP problem can be approximated by a pure combinatorial problem, namely the network inhibition problem. With this reduction, we directly seek the values of discrete variables in the formulation *without* solving the nonlinear equations, simplifying the problem complexity in both theoretical and practical senses. It is worth noting that our reduction respects the nonlinearity of the problem and does not linearize the power flow equations. It is the special combinatorial structure in this nonlinear problem that enables our reduction to a combinatorial problem.

Identification of multiple contingencies has recently drawn much interest from both the optimization and power systems communities. Salmeron, Wood, and Baldick [28] employed a linearized power flow model and used a bilevel optimization framework along with mixed-integer programming to analyze the security of the electric grid. The critical elements of the grid were identified by maximizing the long-term disruption in the power system operation. The bilevel optimization framework has also been used by Arroyo and Galiana [20]. In all of these formulations the optimization framework appears promising for such types of problems where the critical system elements that make the system vulnerable to failures must be identified. Donde et al. [11] proposed a method that connected the feasibility boundary of power flow equations with spectral graph theory, when voltages are fixed at their nominal values, and only active power flow constraints are considered. Later, Donde et al. [12] extended their approach to include reactive power and proposed a mixed integer nonlinear programming formulation to identify the most significant blackout that can be caused by a specified number of lines or to identify the minimum number of lines to cause a blackout of specified severity. More recently, Lesieutre et al. [21, 22] approached this problem from a graph theoretical perspective, by looking for subgraphs in a given graph that are loosely connected to the rest of the graph and have a significant load/generation mismatch. Grijalva and Sauer [17, 18] related topological cuts in the power network with the static collapse based on branch complex flows. He et al. [19] used a voltage stability margin index to identify weak locations in a power network. Bienstock and Mattia used the direct current power flow model and mixed integer linear programming to find the most cost-effective way to increase edge capacities to avoid cascading outages for a given set of failure scenarios [3]. Oliviera et al. have used similar models and techniques to study how to add power lines to improve system resilience [23]. Pinar, Reichert, and Lesieutre proposed a method to compute criticality of lines that can be used in a branching method [26]. In addition to these largely static analyses, the study of system dynamics for cascading events has also drawn interest. In [4, 6, 8] Dobson et al. used a long-term model of the grid to study how failure of a component affects other components in the system, to reveal failure statistics consistent with those observed in the power grid. The same authors have also studied probabilistic models with the aim to better understand cascade propagation [5, 9, 10].

The remainder of this article is organized as follows. Section 2 reviews matrix representations of graphs and the basics of spectral graph theory that are relevant to this article. In section 3, we discuss power flow equations, introduce load shedding, and present a bilevel MINLP formulation for the power network vulnerability analysis problem. Section 4 presents the KKT conditions for the load shedding problem and describes an augmented system for which we prove the MFCQ conditions are satisfied. Further analysis of the feasibility conditions in section 5 reveal a special combinatorial structure in a feasible solution to the bilevel MINLP formulation of the problem. We exploit this combinatorial structure to approximate the original formulation with a pure combinatorial problem in section 6, where we describe the network inhibition problem and its integer programming formulation. We conclude with section 7.

2. Graphs and matrices. Matrix representations of graphs have long been used to apply algebraic techniques to analyze graphs. Here we review the *arc-node incidence* matrix and the *Laplacian* matrix as two of the commonly used representations for graphs. The arc-node incidence matrix of a graph is used in flow problems, and we will use this representation to present power flow equations. The Laplacian matrix for graphs, on the other hand, underlies spectral graph theory, which can be used to analyze the connectedness of graphs. Let $G = (V, E)$ be a graph with n vertices and m edges. We use (v_i, v_j) to denote an edge that goes from vertex v_i to vertex v_j. In this article, we define the arc-node incidence matrix A of this graph as an $m \times n$ matrix, where the jth column of A represents the jth vertex, v_j, and the ith row represents the the ith edge, e_i, in G. Each row has only two nonzeros at the columns that represent the end vertices of the respective edge. The entry is -1 or 1, depending on whether the respective edge is directed from or to the corresponding vertex, respectively. To avoid confusion with the notation, note that the transpose of this matrix, where rows and columns represent vertices and edges, respectively, is more commonly used. Our choice here is for consistency with the power systems literature.

Formally, we use a_{ij} to denote the matrix entry at the ith row and the jth column of A, which is defined as follows:

$$a_{ij} = \begin{cases} -1, & \text{if} \quad e_i = (v_j, u) \in E, \\ 1, & \text{if} \quad e_i = (u, v_j) \in E, \\ 0, & \text{otherwise.} \end{cases}$$

The arc-node incidence matrix A of the graph in Figure 2.1 is as follows:

$$A = \begin{pmatrix} -1 & 1 & & & & \\ -1 & & 1 & & & \\ & 1 & -1 & & & \\ & -1 & & 1 & & \\ & -1 & & & 1 & \\ & & -1 & & 1 & \\ & & & -1 & & 1 \\ & & & & -1 & 1 \end{pmatrix}.$$

The Laplacian of a graph $G = (V, E)$ is an $n \times n$ matrix, where each row and column represents a vertex in the graph. The diagonal entry is equal to the degree of the associated vertex. An off-diagonal entry is -1, if the associated vertices of the row and column are connected in the graph, and 0 otherwise. Formally, let d_i denote the degree of vertex v_i, and let l_{ij} denote the entry of the Laplacian matrix at the ith row and the jth column, which we define as follows:

$$l_{ij} = \begin{cases} d_i, & \text{if} \quad i = j, \\ -1, & \text{if} \quad (v_i, v_j) \in E \quad \text{or} \quad (v_j, v_i) \in E, \\ 0, & \text{otherwise.} \end{cases}$$

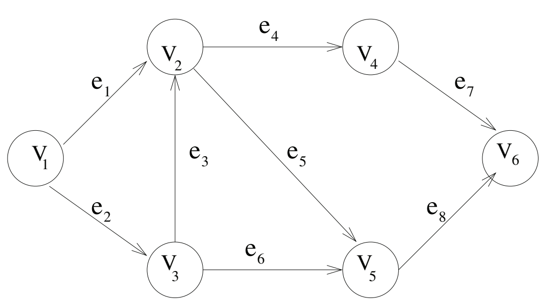

FIG. 2.1. *A sample directed graph.*

The Laplacian of the graph in Figure 2.1 is

$$L = \begin{pmatrix} 2 & -1 & -1 & & & \\ -1 & 4 & -1 & -1 & -1 & \\ -1 & -1 & 3 & & -1 & \\ & -1 & & 2 & & -1 \\ & -1 & -1 & & 3 & -1 \\ & & & -1 & -1 & 2 \end{pmatrix}.$$

We note that L can also be defined as

$$L = A^T A, \tag{2.1}$$

where A is the arc-node incidence matrix of the graph. This property holds regardless of the directions of edges in G. It is possible to add edge weights to the definition of Laplacian of a graph. In this case, the diagonal entry becomes the sum of weights of edges adjacent to the respective vertex, as opposed to the degree of this vertex, and the negative of the edge weight replaces "-1" as the off-diagonal entries. In this case, (2.1) can be rephrased as

$$L_w = A^T D_w A, \tag{2.2}$$

where D_w is a diagonal matrix so that the ith diagonal entry is the weight of edge e_i, and L_w is the weighted Laplacian. Observe that if an arc is removed in the graph, then the corresponding L_w is obtained by setting the corresponding diagonal entry of D_w to zero.

The Laplacian of a graph is the basic element of spectral graph theory. Let $\lambda_0 \leq \lambda_1 \leq \cdots \leq \lambda_{n-1}$ be the eigenvalues of L. The Laplacian matrix is symmetric and semidefinite, and thus all eigenvalues are real and nonnegative. It is easy to see that $\lambda_0 = 0$, since all rows and columns of L add up to zero, and thus the vector e, whose entries are all the same and nonzero, is a singular vector for L. The smallest nontrivial eigenvalue λ_1 is more interesting due to its applications. Fiedler called λ_1 the *algebraic connectivity* of G [14], as it provides a metric for the connectedness of a graph. If the graph inherently involves two loosely coupled subgraphs, then λ_1 will be small. Fiedler also proved that λ_1 will decrease as we remove edges from the original graph, and it will be zero when the graph is decoupled into two disconnected components. A fundamental result in spectral graph theory generalizes this observation so that the multiplicity of the eigenvalue 0 gives the number of connected components in G.

LEMMA 2.1. *Let L be the Laplacian of graph G, and let $\lambda_0 \leq \lambda_1 \leq \cdots \leq \lambda_{n-1}$ be its eigenvalues. If $\lambda_i = 0$ and $\lambda_{i+1} \neq 0$, then G has exactly $i + 1$ connected components.*

The eigenvectors for the eigenvalue 0 reflect the connected components, as vertices of the same component will have the same value for their entries on these eigenvectors.

3. Problem formulation. Our focus in this work is to identify simple events that can trigger a cascading event, not to analyze consequences of cascading. Cascading events start with a significant disturbance to the system and continue with failures of other system components, as these components are pushed beyond their capabilities, while the system is trying to avert a blackout. It will be the initial significant disturbance that we seek in this work, and thus we focus on static power flow analysis. Below, we first describe our power flow model and then describe how we measure the significance of an event. Finally, we cast the power grid vulnerability problem as a bilevel MINLP problem.

3.1. Power system model. We consider a lossless power system with a connected network of m buses (nodes) and n lines (edges). We assume the voltages at the buses are fixed, and thus the dependence of real power injections at buses on the phase angle variables θ can be fully described by active power constraints, making the reactive power constraints unnecessary. The power flowing through the lines can be expressed as

$$P_{line} = B \sin(A\theta),$$

where P_{line} is a vector of power flows over the lines, B is a diagonal matrix whose diagonal entries correspond to line admittances, A is a node-arc incidence matrix that represents the power network, and $\sin(A\theta)$ denotes a vector whose ith component is $\sin((A\theta)_i)$. A vector of power injections P is then obtained by adding the power flowing out of the buses into the network.

$$A^T B \sin(A\theta) - P = 0, \tag{3.1}$$

with $A\theta$ taking values between $-\pi/2$ and $\pi/2$, as required for steady state stability. We will refer to (3.1) as the *power flow equations*. Details and generalizations of this model can be found in [16, 29].

Here, we will work with a given topology of the power grid and investigate the endurance of the grid to changes in topology. To extend the power flow equations for changing topologies, we introduce binary-valued line parameters γ_i that indicate whether the ith line is in service. That is,

$$\gamma_i = \begin{cases} 0, & \text{if the line is in service,} \\ 1, & \text{if the line is out of service.} \end{cases}$$

For simplicity of notation, we define $\Gamma = \operatorname{diag}(1 - \gamma)$ as a diagonal matrix, whose ith diagonal entry is $1 - \gamma_i$. The power flow model (3.1), now with line parameters, can be expressed as

$$F(A, B, \Gamma, \theta, P) = A^T B \Gamma \sin(A\theta) - P = 0. \tag{3.2}$$

Removing lines from the network has the effect of collapsing the feasibility region of solutions to (3.2), as illustrated in Figure 3.1. This figure shows the schematic view of (3.2) in P space. When all lines under consideration are in service, the curve shown

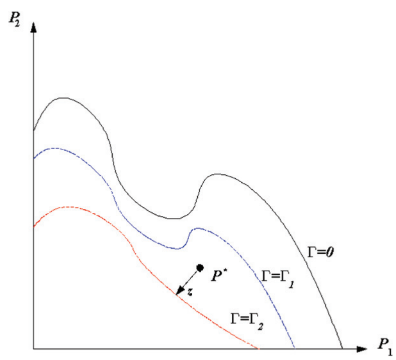

FIG. 3.1. *Space of real power injections showing feasibility boundaries for various line statuses. $\Gamma = 0$ correspond to the initial feasibility boundary. Γ_1 and Γ_2 include broken power lines and illustrate how the feasibility region collapses with missing lines.*

as a solid line represents a feasibility boundary for the power flow constraints. In the normal case, the system operating point lies within the feasible region. When a line is removed from service, the feasibility boundary comes closer to the operating point (marked as P^* in Figure 3.1), increasing the system's vulnerability to failure. Eventually, the removal of a line pushes the boundary past the operating point (dotted-lined curve), making system operation infeasible due to the absence of a solution of (3.2). This implies a blackout, and averting this blackout requires changing the loads and generation, and hence moving the operating point P^*, which we discuss next.

3.2. Measuring the severity of a blackout. Load shedding means cutting off supply to some loads when the demand becomes greater than the supply. While its common use is for high energy–demand times, broken power lines create subregions for which the demand cannot be met with the reduced transmission capability of the grid, even though supply is available in other parts of the system. Here, we use load shedding to minimally change load and generation to restore feasibility to the system to avert a blackout. From a mathematical point, a blackout corresponds to the current operating point P being outside of the feasibility region, and load shedding corresponds to finding the closest point to P on the feasibility boundary, subject to some engineering constraints. The vector Z, which moves the operating point P to the feasibility boundary, describes how to restore feasibility with minimum changes in loads, and the L_1-norm of this vector can be used as an estimate of the size of a blackout.

Suppose the nodes of the system are divided into two groups: generator nodes N^g and load nodes N^l. For simplicity of presentation, we will reorder all the vectors and matrices so that generator nodes precede load nodes. Let $Z^T = ((Z^g)^T, (Z^l)^T)$ be the vector that represents the change in power assignment to nodes, where Z^g and Z^l denote changes in generations and loads, respectively. By convention,

$$P_i^l \leq 0 \quad \text{for all load nodes,}$$
$$P_i^g > 0 \quad \text{for all generation nodes.}$$

This requires

$$Z_i^g \leq 0 \quad \text{and} \quad Z_i^l \geq 0$$

for load shedding. Since we assume a lossless system, the decrease in generation should match the decrease in consumption (i.e., $e^T Z^g = -e^T Z^l$); thus it is sufficient to look at only one of Z^g and Z^l to measure the total volume of load shed. An optimal load shedding strategy can be computed by solving the following optimization problem.

$$\min_{Z} \quad -e^T Z^g, \tag{3.3}$$
$$\text{s.t.} \quad F(A, B, \Gamma, \theta, P + Z) = 0, \tag{3.4}$$
$$P^l \leq P^l + Z^l \leq 0, \tag{3.5}$$
$$0 \leq P^g + Z^g \leq P^g, \tag{3.6}$$
$$-\pi/2 \leq A\theta \leq \pi/2. \tag{3.7}$$

Here, (3.4) corresponds to the power flow equation. Constraints (3.5) and (3.6) guarantee that load and generation do not increase and remain as load and generation, respectively. The last constraint (3.7) ensures steady state stability. The minus sign in the objective (3.3) is because Z^g are nonpositive as they represent how much generation will be cut.

3.3. Power network vulnerability analysis as a bilevel MINLP problem. The power network vulnerability analysis problem can be posed as a bilevel mixed integer nonlinear optimization problem, where in the outer level we look for the critical lines, which corresponds to the combinatorial part of the problem, and in the inner level we measure the blackout severity by solving the load shedding problem, which corresponds to the nonlinear part of the problem. For a formal definition, let $LS(A, B, \Gamma, \theta, P)$ denote an instance of the load shedding problem in (3.3)–(3.7), and let $\arg\min LS(A, B, \Gamma, \theta, P)$ denote an optimal solution to this problem. The power network vulnerability analysis problem can then be defined as follows:

$$\min_{\theta,\gamma,Z} \quad e^T\gamma, \tag{3.8}$$

$$\text{s.t.} \quad Z = \arg\min LS(A, B, \Gamma, \theta, P), \tag{3.9}$$

$$-e^T Z^g \geq S, \tag{3.10}$$

$$\gamma_i \in \{0, 1\} \quad \text{for} \quad i = 1, 2, \ldots, m, \tag{3.11}$$

where $S > 0$ is a specified severity. In general, bilevel optimization problems are hard to solve and in the next two sections, we will present approximations to this formulation.

4. Reduction to a single level MINLP. This section analyzes the necessary conditions of optimality for the inner optimization problem, which measures the blackout severity. We first describe the KKT conditions and then the MFCQ conditions for the load shedding problem. Then we discuss the structure of the Jacobian of the power flow equations, which we use to build an augmented system for which MFCQ conditions are satisfied. Finally, we present a single level MINLP formulation for the power grid vulnerability analysis problem, which approximates the bilevel MINLP formulation in the previous section, by replacing the inner optimization problem with its KKT conditions. In [12], a similar formulation is presented for a full power flow model with active and reactive power equations, and a slightly different load shedding model.

4.1. KKT conditions for the load shedding problem. The Lagrangian $\mathcal{L}$ corresponding to (3.3)–(3.7) is

$$\begin{aligned}\mathcal{L} = &-e^T Z^g + \lambda^T F(\theta, P + Z) + \mu_1^T(-Z^l) + \mu_2^T(P^l + Z^l) + \mu_3^T(-P^g - Z^g) \\ &+\mu_4^T(Z^g) + \mu_5^T(-A\theta - \pi/2) + \mu_6^T(A\theta - \pi/2),\end{aligned} \tag{4.1}$$

where $\mu_1, \ldots, \mu_6$, and λ are vectors of Lagrange multipliers. KKT conditions for the problem in (3.3)–(3.7) are as follows:

$$\nabla_Z \mathcal{L} = \begin{pmatrix} -e \\ 0 \end{pmatrix} + \lambda^T \frac{\partial F}{\partial Z} + \begin{pmatrix} \mu_4 - \mu_3 \\ \mu_2 - \mu_1 \end{pmatrix} = 0, \tag{4.2}$$

$$\nabla_\theta \mathcal{L} = \lambda^T \frac{\partial F}{\partial \theta} + A^T(\mu_6 - \mu_5) = 0, \tag{4.3}$$

$$F(A, B, \Gamma, \theta, P + Z) = 0, \tag{4.4}$$

$$\mu_1.(-Z^l) = 0, \tag{4.5}$$

$$\mu_2.(P^l + Z^l) = 0, \tag{4.6}$$

$$\mu_3.(-P^g - Z^g) = 0, \tag{4.7}$$

$$\mu_4.Z^g = 0, \tag{4.8}$$

$$\mu_5.(-\pi/2 - A\theta) = 0, \tag{4.9}$$

$$\mu_6.(A\theta - \pi/2) = 0, \tag{4.10}$$

$$\mu_1, \ldots, \mu_6 \geq 0. \tag{4.11}$$

The notation "." in (4.5)–(4.10) is used to indicate component-wise multiplication of associated vectors. (4.2) and (4.3) correspond to the partial derivatives of $\mathcal{L}$ with respect to Z and θ, respectively, and (4.5)–(4.10) correspond to inequality constraints (3.5)–(3.7). Optimal solutions to problem (3.3)–(3.7) satisfy the KKT conditions (4.2)–(4.11).

4.2. Mangasarian–Fromovitz constraint qualification conditions. MFCQ conditions correspond to the set of possible KKT multipliers being bounded, and they can be stated as follows. Given an optimization problem

$$\begin{aligned} \min \quad & f(x) \\ \text{s.t.} \quad & C_i(x) = 0 \quad i \in E, \\ & C_i(x) \geq 0 \quad i \in I, \end{aligned}$$

let x^* be an optimal solution, and let $A(x^*)$ be the corresponding set of active constraints. There exists a vector $w \in R^n$ such that

$$\nabla C_i(x^*)^T w > 0 \qquad \forall i \in A(x^*) \cap I, \tag{4.12}$$

$$\nabla C_i(x^*)^T w = 0 \qquad \forall i \in E, \tag{4.13}$$

and the set of equality constraint gradients $\nabla C_i(x^*), i \in E$ is linearly independent.

For our problem, let $w = (w_\theta^T, w_z^T)^T$. The constraints (3.7) due to active inequality constraints on angular differences can be simplified as follows:

$$w_\theta^i < w_\theta^j \quad \text{if} \quad \theta_i^* - \theta_j^* = \pi/2, \text{ and nodes } i \text{ and } j \text{ are connected.} \tag{4.14}$$

The constraints due to active load shedding constraints (3.5)–(3.6) can be phrased as follows:

$$w_z^i < 0 \quad \text{if} \quad i \text{ is a load and } Z_i^l = -P_i^l, \tag{4.15}$$

$$w_z^i > 0 \quad \text{if} \quad i \text{ is a load and } Z_i^l = 0, \tag{4.16}$$

$$w_z^i < 0 \quad \text{if} \quad i \text{ is a generator and } Z_i^g = 0, \tag{4.17}$$

$$w_z^i > 0 \quad \text{if} \quad i \text{ is a generator and } Z_i^g = -P_i^g. \tag{4.18}$$

Finally, we have the MFCQ conditions due to the equality constraints. Let $F(x^*)$ represent the power flow equations at point x^*. Then we have

$$\nabla C_i(x^*) = \left(\frac{\partial F^{*T}}{\partial \theta}, \frac{\partial F^{*T}}{\partial Z} \right)^T = (J^*, I)^T, \tag{4.19}$$

whose rows are linearly independent, due to the embedded identity in the second part of the matrix. Here, we use J^* to refer to the Jacobian of the power flow equation with respect to the phase angle variables evaluated at x^*.

Using the identity matrix embedded in (4.19), we can merge this set of constraints with that of (4.15)–(4.18) as follows:

$$(Jw_\theta)^i > 0 \quad \text{if} \quad v_i \text{ is a generator with no power shed,} \tag{4.20}$$

$$\text{or} \quad v_i \text{ is a load cut down to 0.} \tag{4.21}$$

$$(Jw_\theta)^i < 0 \quad \text{if} \quad v_i \text{ is a load with no reduction,} \tag{4.22}$$

$$\text{or} \quad v_i \text{ is a generator cut down to 0.} \tag{4.23}$$

In section 4.4 we will use these results to describe an augmented system for which the described MFCQ conditions are satisfied.

4.3. Structure of the Jacobian of the power flow equations. The Jacobian J of power flow equations in (3.2) with respect to θ is

$$J = \frac{\partial F}{\partial \theta} = A^T B\Gamma \operatorname{diag}(\cos(A\theta))A, \tag{4.24}$$

where $\operatorname{diag}(\cos(A\theta))$ and Γ are diagonal matrices whose ith entries are $\cos((A\theta)_i)$ and $1 - \gamma_i$, respectively. Observe that B, Γ, and $\operatorname{diag}(\cos(A\theta))$ are all diagonal matrices with nonnegative diagonal entries, since γ is a vector of binary variables and the angular differences represented by $A\theta$ are in the $[-\pi/2, \pi/2]$ range; hence $0 \leq \cos((A\theta)_i) \leq 1$. Thus the Jacobian is identical in structure to a weighted Laplacian in (2.2).

When the diagonal entries in $B\Gamma \operatorname{diag}(\cos(A\theta))$ are all nonzero, J has only a single zero eigenvalue, since the network under consideration is initially connected. It is worth noting that when the power flow equation for a reference bus is removed from (3.2), along with its variable θ, the resulting reduced order Jacobian does not have a zero eigenvalue and is singular only when the operating point lies on the feasibility boundary [2]. We preserve the network structure by retaining the reference bus in order to be able to draw direct analogies with spectral graph theory. In our formulation, the Jacobian J is always singular with a single zero eigenvalue and the corresponding eigenvector $e = [1, 1, \ldots, 1]^T$.

Recall from section 2 that removal of an edge appears in the weighted Laplacian as a zero weight assignment to this edge. In the Jacobian, J in (4.24), this happens when $\gamma_i = 1$, which corresponds to removal of a line from the network, or when the angular difference for a line is $\mp\pi/2$, which corresponds to capacity of a line being fully utilized. The second smallest eigenvalue λ_1 becomes zero when the operating point lies on the feasibility boundary. From spectral graph theory, we know that $\lambda_1 = 0$ means that the graph has at least two connected components, as discussed in section 2.

The power flow Jacobian J is analogous to the *residual* graph for flow problems in graph theory, which represents the incremental transmission capability of the network. In a residual graph, edge capacities correspond to unused edge capacities or used edge capacities on the reverse arc. The incremental transmission capability of the system is measured by the total flow capacity from the source to the terminal in the residual graph. If a group of vertices is disconnected from the source, then we cannot send any more flow to these vertices. An optimal solution (i.e., the maximum flow) is defined by an instance of this, where the source and the terminal are disconnected in the residual graph. In power systems, the flow between two nodes is determined by the sine of the angular difference between the two nodes, thus the cosine of this angular difference can be viewed as the residual capacity of this line. When the operating point is on the boundary of feasibility, there will be a nonempty set of load change vectors that the system will not be able to respond to, which is reflected by the multiplicity of the zero eigenvalue being more than 1. By Lemma 2.1, the system is divided into at least two subgroups that are connected by either saturated lines with angular difference at $\mp\pi/2$ or removed lines due to the γ variables.

4.4. An augmented system that satisfies the MFCQ conditions. This section proves that the MFCQ conditions are satisfied for an augmented system.

In the augmented system, for each node v we add two auxiliary nodes (one generator v_g and one load v_l) and two auxiliary edges (corresponding to high impedance lines) that connect auxiliary nodes v_g and v_l to v. We set the generation and the load on these auxiliary nodes to be equal to the same infinitely small quantity. The small values ensure that the generation/load distribution in the system is not affected, and thus the vulnerabilities remain the same. And the high impedance lines guarantee that the angular differences on these lines will never reach $\pi/2$.

We also augment the load shedding problem such that the objective function contains the load nodes as well as the generation nodes, which only affects the value of an optimal solution, but not the solution itself. We further adjust the objective function so that the generation/load shedding on the auxiliary nodes are penalized more than those of the other nodes. Observe that it is always possible to transfer the power from the generator to the load of an auxiliary pair with no effect on the rest of the system. When we set the penalty function high enough, there will be no load shedding in the auxiliary nodes, which leads to a two-way relation between the optimal solutions to the original and the augmented systems. An optimal solution to the original problem can be transformed to an optimal solution for the augmented system, by changing the flow on the auxiliary edges to transfer power from the generator to the load of each pair. Symmetrically, an optimal solution for the augmented system defines an optimal solution for the original system.

Our proof is constructive. In the first step of our construction, we construct a solution that satisfies (4.14). The second step guarantees that (4.20)–(4.23) are satisfied for all auxiliary vertices. Then at the third step, (4.20)–(4.23) are satisfied for the remaining nodes. Updates at each step preserve the feasibility of conditions of previous steps. Explanation of these steps follow.

Step 1. Assigning $w^i = \theta^i$ will automatically satisfy (4.14) for the whole system.

Step 2. At the second step, we adjust w values for the auxiliary vertices to satisfy (4.20)–(4.23). For an auxiliary generator, we only need to worry about (4.20), since by construction, load shedding does not affect the auxiliary nodes. Similarly for auxiliary loads, we only need to worry about (4.22). Consider an auxiliary generator and its entry w^i, for which (4.20) is not satisfied. The corresponding row in the Jacobian has two entries: a positive entry on the diagonal and a negative entry on the column of the vertex it is connected to, which add up to 0. By choosing the w^i value of the auxiliary generator larger than that of the node it is connected to, we can guarantee that (4.20) is satisfied. Symmetrically, for an auxiliary load vertex, choosing its w^i, smaller than that of the node it is connected to satisfies (4.22). At the end of this intermediate step, (4.20)–(4.23) are satisfied for all auxiliary nodes.

Step 3. By our analysis in section 4.3, we know that the $(Jw)^i$ value of a node can be increased or decreased by, respectively, decreasing or increasing the w^j values of any of its neighbors connected to this node with an unsaturated edge. Now consider a node, for which one of the (4.20)–(4.23) conditions is not satisfied. That is, we can linearly increase or decrease the $(Jw)^i$ value by, respectively, increasing the w^j value of its auxiliary generator or decreasing the w^j value of its auxiliary load. Further increasing or decreasing the w^j values will not violate (4.20) or (4.22) and will not affect any other nodes. Therefore, we can adjust the w values for the auxiliary nodes to satisfy all constraints. And this concludes our construction.

Changing our formulation for the augmented system requires redefining A, B, and P, which describe the system and vector e in (3.10). For simplicity and clarity of the presentation, however, we will not change the notation in the remainder of the paper.

4.5. A MINLP formulation. The power network vulnerability analysis problem can be formulated as the following MINLP problem:

$$\min_{\theta,\gamma,z} \quad e^T\gamma, \tag{4.25}$$

$$\text{s.t.} \quad A^T B\Gamma \sin(A\theta) - (P + Z) = 0, \tag{4.26}$$

$$-\pi/2 \le A\Gamma\theta \le \pi/2, \tag{4.27}$$

$$P_l \le P^l + Z^l \le 0, \tag{4.28}$$

$$0 \le P^g + Z^g \le P_g, \tag{4.29}$$

$$-e^T Z^g \ge S, \tag{4.30}$$

$$\begin{pmatrix} -e \\ 0 \end{pmatrix} - \lambda + \begin{pmatrix} \mu_4 - \mu_3 \\ \mu_2 - \mu_1 \end{pmatrix} = 0, \tag{4.31}$$

$$J\lambda + A^T\Gamma(\mu_6 - \mu_5) = 0, \tag{4.32}$$

$$\mu_1.(-Z^l) = 0, \tag{4.33}$$

$$\mu_2.(P^l + Z^l) = 0, \tag{4.34}$$

$$\mu_3.(-P^g - Z^g) = 0, \tag{4.35}$$

$$\mu_4.Z^g = 0, \tag{4.36}$$

$$\mu_5.(\pi/2 + A\Gamma\theta) = 0, \tag{4.37}$$

$$\mu_6.(A\Gamma\theta - \pi/2) = 0, \tag{4.38}$$

$$\mu_1, \ldots, \mu_6 \ge 0, \tag{4.39}$$

$$\gamma_i \in \{0, 1\} \quad \text{for} \quad i = 1, 2, \ldots, m. \tag{4.40}$$

Here, (4.26) and (4.27) guarantee that there is a feasible solution to the power flow equations at $P + Z$, and (4.30) enforces that the resulting blackout is no smaller than a specified severity S. Inequalities (4.28) and (4.29) are the load shedding constraints, and (4.31)–(4.39) correspond to the KKT conditions, so that Z satisfies the necessary conditions for an optimal solution for the load shedding problem. In these equations, we have substituted $\frac{\partial F}{\partial Z} = I$, and $J = \frac{\partial F}{\partial \theta}$. Finally, (4.40) correspond to discrete line parameters, which indicate whether a line is cut ($\gamma_i = 1$) or active ($\gamma_i = 0$).

This formulation reduces the bilevel optimization problem to a single-level MINLP problem. Next, we will analyze the structure of an optimal solution to the problem (4.25)–(4.40) to approximate it as a pure combinatorial problem, with a lower complexity, both in theory and in practice.

5. Analysis of the formulation.

In this section, we analyze the structure of a feasible solution to our MINLP formulation to reveal a special combinatorial structure that can be exploited to approximate our MINLP formulation with a pure combinatorial problem. While we will be referring to the single-level MINLP formulation, our analysis does not depend on reducing the bilevel optimization problem to a single-level optimization problem. Our arguments are based on optimality conditions for the load shedding problem, but not necessarily on replacing an optimization problem with necessary conditions for its optimality. Our reduction enables us to directly seek the values of binary variables in the problem, *without* solving the nonlinear equations.

5.1. Structure of a feasible solution.

An analysis of the Lagrangian multipliers sheds light onto the structure of a solution for problem (4.25)–(4.40). We will show that the system is decomposed into a generation-rich region and a load-rich region. Then, we will study the flow on the lines between these regions.

5.1.1. Decomposition into load- and generation-rich regions.

Let $\lambda = ({\lambda^g}^T, {\lambda^l}^T)^T$ be partitioned into variables for generator and load nodes, so that we can split (4.31) into two equations.

$$-e - \lambda^g + \mu_4 - \mu_3 = 0, \tag{5.1}$$

$$0 - \lambda^l + \mu_2 - \mu_1 = 0. \tag{5.2}$$

Consider a generator vertex and the associated Lagrangian multiplier λ_i^g. If $\lambda_i^g < -1$, then by (5.1), the corresponding μ_3 variable must be positive. This requires $Z_i^g + P_i^g = 0$ by (4.35), which means the generation at this node will be zero after load shedding. If $\lambda_i^g = -1$, then the corresponding μ_3 and μ_4 variables must be equal by (5.1). This is possible only when they are both zero, since μ_3 and μ_4 correspond to lower and upper bounds on $P^g + Z^g$. In this case, neither bound is binding and the generation after load shedding is anything in the range $[0, P_i^g]$. Finally, if $\lambda_i^g > -1$, then by (5.1), the corresponding μ_4 variable must be positive. This requires $Z_i^g = 0$ by (4.35), which means that there will be no decrease in the generation at this node.

We can do a similar analysis for the load nodes. Consider a load vertex and the associated Lagrangian multiplier λ_i^l. If $\lambda_i^l > 0$, then by (5.2), the corresponding μ_2 variable must be positive. This requires $Z_i^l + P_i^l = 0$ by (4.34), which means the load at this node will be zero after load shedding. If $\lambda_i^l = 0$, then the corresponding μ_1 and μ_2 variables must be equal by (5.2). This is possible only when they are both zero, since μ_1 and μ_2 correspond to lower and upper bounds on $P^l + Z^l$. In this case, neither bound is binding and the load after shedding is anything in the range $[0, P_i^l]$. Finally, if $\lambda_i^l < 0$, then by (5.2), the corresponding μ_1 variable must be positive. This requires $Z_i^l = 0$ by (4.35), which means that there will be no decrease in the load at this node.

This yields the following load shedding model. For generation nodes,

$$Z_i^g = 0 \qquad \text{if} \quad \lambda_i > -1, \tag{5.3}$$

$$0 \le Z^g + P^g \le P^g \qquad \text{if} \quad \lambda_i = -1, \tag{5.4}$$

$$Z_i^g = -P_i^g \qquad \text{if} \quad \lambda_i < -1. \tag{5.5}$$

And for loads

$$Z_i^l = 0 \quad \text{if} \quad \lambda_i < 0, \tag{5.6}$$

$$P^l \le Z^l + P^l \le 0 \quad \text{if} \quad \lambda_i = 0, \tag{5.7}$$

$$Z_i^l = -P_i^l \quad \text{if} \quad \lambda_i > 0. \tag{5.8}$$

Observe that not all $\lambda_i \ge 0$, since that requires $Z^g = 0$ for all generation nodes, which contradicts the blackout severity constraint, $-e^t Z^g \ge S$. Similarly, not all $\lambda_i < 0$, since that requires $Z^l = 0$ for all loads. Since we have a lossless system, $Z^l = 0$ implies $Z^g = 0$, which again contradicts the blackout severity constraint.

Based on these observations, we can decompose the system into two regions based on their Lagrangian multipliers. Let the first group be composed of nodes for which $\lambda_i < 0$, and the second group be composed of the remainder for which $\lambda_i \ge 0$. For the first region ($\lambda_i < 0$), we know by (5.6) that the loads should not be decreased while the generation can be decreased as necessary. For the second region ($\lambda_i \ge 0$), we know by (5.3) that the generation should not be decreased, whereas the loads can be decreased as necessary. Thus the Lagrangian multipliers give a decomposition of the system into two regions: a *generation-rich* region, P_1, defined by $\lambda_i < 0$, where only the generation can be decreased and loads remain the same, and *load-rich* region, P_2, defined by $\lambda_i \geq 0$, where only the loads can be decreased and the generation remains the same.

The reason for a blackout is the failure to transmit power from the generation-rich part to the load-rich part, and moreover, the best way to restore the system to feasibility is to decrease the generation in the generation-rich part and the load in the load-rich part.

5.1.2. Flow between the two regions. In the previous section, we showed that at a feasible solution to (4.25)–(4.40), the system will be decomposed into a generation-rich region, P_1, and a load-rich region, P_2. Now, we study the flow between these two regions by investigating (4.32) and show that there is at least one line between the two regions that uses its maximum capacity to carry power from the generation-rich side to the load-rich side.

For simplicity of presentation, we assume all vectors are permuted so that the nodes in the generation-rich region are ordered before those in the load-rich region, and the same permutation is applied to matrices symmetrically. Let $\lambda = ({\lambda^1}^T, {\lambda^2}^T)^T$, so that λ^1 corresponds to the nodes in the generation-rich region ($\lambda^1_i < 0$), and λ^2 corresponds to the nodes in the load-rich region ($\lambda^2_i \geq 0$). Then (4.32) can be rewritten as

$$\begin{pmatrix} J_{11} & J_{12} \\ J_{21} & J_{22} \end{pmatrix} \begin{pmatrix} \lambda^1 \\ \lambda^2 \end{pmatrix} + A^T\Gamma(\mu_6 - \mu_5) = 0, \tag{5.9}$$

where J_{11}, J_{12}, J_{21}, and J_{22} are submatrices of J that conform with $({\lambda^1}^T, {\lambda^2}^T)^T$. Recall that J is symmetric and diagonally dominant, with the only nonnegative entries on the diagonals, and the sum of absolute values of the remaining entries on a column/row is equal to the diagonal entry. Thus, $e^T J_{11}\lambda^1 \leq 0$, where the equality is satisfied only when $J_{21} = M_0$, where we use M_0 to denote a matrix of all zeros. Observe that J_{12} and J_{21} matrices correspond to the lines between the two regions, and their nonzeros correspond to lines that are neither cut ($\gamma_i = 1$) nor saturated due to the angular difference being $\mp\pi/2$.

In section 5.1.3 we discuss the special case where $J_{12} = J_{21} = 0$. In general, $J_{12} = J_{21}^T \neq 0$; thus there may be unsaturated lines between the two regions. In this case,

$$e^T(J_{11}, J_{12})({\lambda^1}^T, {\lambda^2}^T)^T < 0,$$

since $e^T J_{11}\lambda^1 < 0$, J_{12} is composed of all negative entries, and λ^2 is composed of all nonnegative entries. This means for (5.9) to be satisfied, $A^T\Gamma(\mu_6 - \mu_5) \neq 0$. The Lagrangian multipliers μ_5 and μ_6 are for lower and upper bounds on $A\theta$, and thus only one can be nonzero, when the angular difference at the corresponding line is $\mp\pi/2$. Thus there must be at least one active line ($\gamma_i = 0$) that is saturated. Recall that each column of A^T has one "-1" and one "1"; thus the saturated line that is internal in one of the regions will not help, and we need a saturated line that goes between the two regions.

Assume this line is directed from P_1 to P_2; that is, the column in A^T for this line has its -1 in the generation-rich part and its 1 in the load-rich part. This implies that the corresponding entry in μ_5 needs to be positive, since we need a positive addition to the first part. The Lagrangian multiplier μ_5 can be positive only when the angular difference for this line is $-\pi/2$, which means the power flows from the generation-rich side P_1 to the load-rich side P_2. Symmetrically, if the line is directed from P_2 to P_1

in matrix A^T, then μ_6 needs to be positive, which means angular difference for this line is $\pi/2$, and thus power flows again from the generation-rich side to the load-rich side. This observation does not hold for each line on the boundary, but we know that it holds for at least one boundary line.

5.1.3. Analysis of a special case. In this section we analyze a special case where the Lagrangian multipliers for the constraints on angular differences are set to be zero, i.e., $\mu_5 = \mu_6 = 0$. This corresponds to a degenerate case, and our goal here is to better disclose the combinatorial structure in a solution to (4.25)–(4.40). While our results in the remainder of the paper do not rely on the results in this section, we believe what we present can play an important enabling role for future studies.

The Lagrangian multipliers μ_5 and μ_6 being zero reduces (4.32) to $J\lambda = 0$. As shown in section 5.1.1, all entries of λ cannot be the same; some of them need to be nonnegative, and some need to be negative. This excludes the $\lambda = (1, 1, \ldots, 1)^T$, solution, and thus we need another singular vector for J. By our discussions in section 2, we know that for J to have another singular vector the graph corresponding to J should be decomposed into multiple components, which is possible due to broken and saturated lines. This means in a solution to our problem, the power grid will be decomposed into at least two groups, so that the edges connecting these groups are either cut ($\gamma_i = 1$) or saturated (the angular difference is $\mp\pi/2$). For brevity, we assume there are exactly two groups in the system.

The entries in the associated singular vector λ will reflect this decomposition of the grid and each λ_i will be assigned one of the two real numbers, c_1 and c_2. Let $c_1 < c_2$, and let P_1 be the set of nodes for which $\lambda_i = c_1$ and P_2 be the set of remaining nodes, for which $\lambda_i = c_2$. In section 5.1.1 we showed that there must be some generators, for which $\lambda_i^g \le -1$, and there must be some loads, for which $\lambda_i^l \ge 0$. Assume $c_1 = -1$ and $c_2 = 0$. Note that this choice does not constrain the other variables, and any other solution can only be as good as a solution with $c_1 = -1$ and $c_2 = 0$. The load shedding model in (5.3)–(5.8) still applies, which means that a feasible solution does not decrease the loads on the P_1 nodes and does not decrease the generation on the P_2 nodes. This shows that the λ vector decomposes the system into a generation-rich part P_1 and a load-rich part P_2, as discussed before. The reason for the blackout is the failure to transmit power from the generation-rich part to the load-rich part, since all lines between these two parts are either cut or already operating at their maximum limits. Moreover, the best way to restore the system to feasibility is to decrease the generation in the generation-rich part and the load in the load-rich part.

5.2. Power network vulnerability analysis as a combinatorial problem. A solution to the problem (4.25)–(4.40) not only provides a small set of critical lines but also computes how load can be shed optimally, phase angles at nodes after load shedding, and a decomposition of the system into load- and generation-rich regions. What we really need is only the set of broken lines, i.e., the vector γ. We need to know the L_1-norm of the Z vector is above a specified severity threshold, but we don't need to compute its entries individually.

By our analysis in section 5.1, we know that optimal load shedding requires decreasing the loads in the load-rich region while keeping the generation as is. Symmetrically, we need to cut the generation in the generation-rich region and retain the loads. The total volume to be shed is defined by the load-generation mismatch in a part, and the total flow on the active boundary edges between the two parts. In this model, the blackout severity is a function of the decomposition of the system and depends on the load generation mismatch in the two regions. Therefore, constraint

(4.30) can be satisfied with the right choice of partitioning. Let T denote the total power being transmitted from one part to another in the remaining network after lines are removed. Then $-e^T Z^g$ can be computed as

$$\left(\sum_{\lambda_i<0} P_i\right) - T. \tag{5.10}$$

Here, the summation computes the excess generation in P_1, and since we cannot cut the loads in this part, the generation must be reduced to match the load after the lines leaving this part are loaded maximally.

We know that at a feasible solution, the power grid will be decomposed into two parts as a load-rich region and a generation-rich region. What (5.10) shows is that an optimal solution seeks for a decomposition that maximizes the generation/load mismatch and minimizes the potential power transmission between the two regions, which reveals a combinatorial structure in the problem. This raises an interesting question of whether we can solve problem (4.25)–(4.40) by directly looking for such a decomposition. Below, we discuss how such a decomposition can be used to find an approximation to the MINLP formulation and why this is a good approximation. The big gain here is that the decomposition problem can be formulated as a MILP, as opposed to a MINLP. It should be noted that our reduction is more than merely solving the discrete portion of a MINLP problem in a decomposition algorithm such as Benders decomposition or outer approximation. Our formulation foresees the change in the nonlinear part and directly seeks values of discrete variables in an optimal solution to the MINLP, *without* explicitly solving the nonlinear part.

For a formal definition, let $Lines(P_1, P_2)$ denote the set of lines between parts P_1 and P_2, $Cap(E)$ be the total capacity of lines in set E, and $L(P_1)$ and $G(P_1)$ be the total load and generation in part P_1, respectively. We define the network vulnerability analysis problem as follows.

Let $G = (V, E)$ be a graph with V as the set of nodes (buses) and E as the set of edges (lines), and let S be a specified severity threshold. Find a minimum cardinality subset of edges $C \subseteq E$, so that there exists a partitioning of nodes V into P_1 and $P_2 = V \setminus P_1$, so that

$$G(P_1) - L(P_1) - Cap(Lines(P_1, P_2) \setminus C) \geq S. \tag{5.11}$$

This problem can be solved as the network inhibition problem in graph theory [24], which we address in the next section. There are two reasons for why the combinatorial model is an approximation and not an exact model. Both reasons cause underestimation of the severity of a blackout, and thus a solution to the combinatorial problem will yield a feasible solution to (4.25)–(4.40), but not necessarily an optimal one.

First, we know that a feasible solution involves a decomposition of the system, where only the generation (load) will be shed in the generation (load)-rich region, but we do not know if this holds for an arbitrary decomposition. That is, in a feasible solution, it is sufficient to shed the load or generation to merely match the other, but this is not necessarily the case for all decompositions, as we might have to lower the generation even in the generation-rich region to restore feasibility. This will cause underestimating the blackout severity, as our combinatorial model does not fully capture the complexity of power flow equations. However, this is not as serious a drawback, since we are only looking for significant blackouts and will cut a significant portion of the generation and loads. This translates to a large feasible space for the minimal load shedding problem, within which it is possible to find an instance where only cutting the loads or generation is sufficient.

The second reason why the combinatorial model is not exact is that the total flow between the two parts may be less than the cumulative capacities of the connecting edges. We know that there will be at least one line that uses its maximum capacity to transfer power from the generation-rich side to the load-rich side. And in our analysis of a special case in section 5.1.3, we showed that all lines between the two parts will be saturated. While the cumulative capacity of lines is not always utilized for a given decomposition of the system, the particular decomposition we choose creates a load/generation mismatch, and minimizing the total volume of load shedding requires maximizing the total flow from the generation-rich side to the load-rich side. Thus the goal of load shedding can be considered as maximizing the flow between the two regions. Therefore, what we use as an approximation is an upper bound on the value of a maximization problem that is implicit in the load shedding problem in (3.3)–(3.7).

5.3. Empirical evaluation. In this section, we present an empirical study that shows that the gap between our combinatorial approximation and the original MINLP formulation is small and rapidly closes as the severity of the blackout increases.

In our experiments, we used a slightly modified version of the IEEE 30 bus system [1] as described in [12], where the generator active power injections are modified so that there is no natural power balance in the system, providing a better test case for vulnerability analysis. This modified data set is presented in detail in [12], and the IEEE 30 bus system is illustrated in Figure 5.1. We used the original system, as opposed to the augmented system described in section 4.4.

In this system, the generation-rich lower subsystem (the shaded region in Figure 5.1) is connected to the load-rich upper subsystem with only four lines (lines 28, 29, 30, and 36). Failures among these lines can cause a blackout, as the remaining lines are not sufficient to transfer power from the generation-rich subregion to the load-rich region. These four lines are the source of all significant, nontrivial vulnerabilities in this system. In our experiments, we have looked at five different combinations of line failures, as lines 28, 29, and 30, lines 28, 29, and 36, lines 28 and 29, lines 29 and

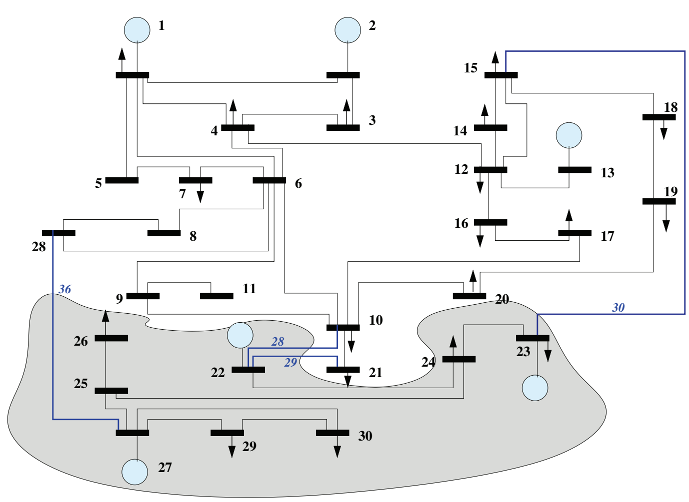

FIG. 5.1. *IEEE 30-bus system.*

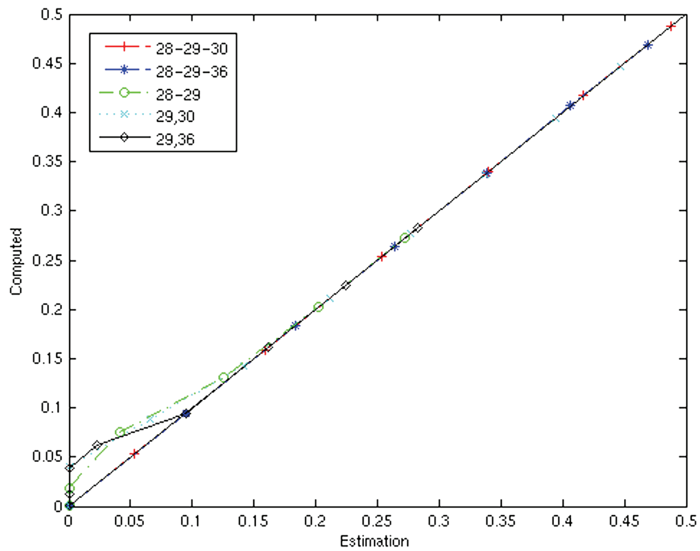

FIG. 5.2. *Accuracy of our combinatorial approximation.*

30, and lines 29 and 36 are cut. To observe how the accuracy of our approximation changes with blackout severity, we increased the generation at the generation-rich region in the lower subsystem and load in the load-rich region. For each of these test cases, the excess generation and load were equally distributed among the generators and load nodes in the respective regions. The results of our experiments are presented in Figure 5.2.

In Figure 5.2, the horizontal axis corresponds to the estimated size of a blackout, which we compute by (5.11). The vertical axis corresponds to the measured size of a blackout, which we compute by solving the optimal load shedding problem in (4.25)–(4.40). To solve the associated nonlinear optimization problem, we used Matlab's `fmincon` with default settings. For each instance, 10 different initial solutions were used, and here we report the best one. Both axes are normalized with respect to the total generation in the system. Each data point corresponds to an experiment with a specified set of broken lines and a generation/load assignment. Experiments with the same set of broken lines are marked with the same sign. Ideally, all points should lie on the main diagonal, which means the estimation is equal to the measurement. However, this does not always hold, either due to our approximation or due to the nonconvexity of the load shedding problem. Note that our combinatorial approximation offers a lower bound on the blackout severity, and the results we obtain by fmincon offer only an upper bound on severity due to the nonconvexity of the problem. The optimal solution value, the real severity, lies between the two. Thus, the gap between the real severity and our approximation is less than what is presented in Figure 5.2.

The results show that our approximation works effectively, especially for blackouts with high severity. The first two sets of broken lines leave only a single line between the generation-rich and load-rich regions. By our analysis, we know that this line will be saturated, and thus our combinatorial approximation will be exact. We can see that the empirical results are consistent with our theoretical studies. The other three cases leave two lines between the two regions. The results show that our combinatorial model underestimates the severity of a blackout (sometimes even misses a blackout, which corresponds to the points on the vertical axis), but the gap between estimated and measured values closes rapidly as the blackout severity increases. Note that we are interested only in severe blackouts, and our combinatorial approximation is accurate for these cases.

6. Solving the network inhibition problem.

In the network inhibition problem, we aim to find the best way to attack a network to minimize its transmission capability. In graph theoretical terms, the network inhibition problem tries to find the most cost-efficient subset of lines, removal of which minimizes the maximum flow on the remaining network. The network inhibition problem naturally involves the maximum flow problem as a subproblem. Below, we first discuss flow networks and define the network inhibition problem. Then we provide an integer programming formulation for this problem and discuss how the power network vulnerability analysis problem can be posed as the network inhibition problem.

6.1. Flow graphs and the maximum flow problem.

A flow network $G = (V, E)$ is defined by a set of vertices V, a set of edges E, where each edge (u, v) has a nonnegative capacity $c(u, v)$, and two special vertices: a *source* s and a *terminal* t. A *flow* in G is a real valued function, $f : E \to \mathcal{R}$. We use $f(u, v)$ to refer to a flow on the edge from vertex u to vertex v. Using a single source and a single terminal vertex provides a standard form for the maximum flow problem, and even if there are multiple vertices with production, a single source vertex s is used, which is connected to all other vertices with production, and the capacity of the connecting edge is equal to the production on that node. Similarly, only a single terminal vertex t is used, which is connected to all other vertices with consumption, and the capacity of the connecting edge is equal to the consumption on that node. We say a flow is feasible if it respects conservation of flow and the capacity constraints on edges. Conservation of flow requires that the total flow into a node is equal to total flow out of that node except for the source and terminal vertices. The value of a flow is defined by the total flow leaving the source, and the maximum flow problem aims to find a feasible flow with maximum value.

A closely related concept to maximum flow is the *minimum cut*. A *cut* in a flow graph is defined by a bipartitioning of vertices V into V_1 and $V_2 = V \setminus V_1$, so that $s \in V_1$ and $t \in V_2$. We say an edge is *in the cut* if one of its end vertices is in V_1 and the other is in V_2. The *capacity* of a cut is defined as the sum of capacities of the edges on the cut, and a minimum cut is one with minimum capacity among all the cuts. It is easy to see that the capacity of any cut is an upper bound on the value of a maximum flow, since the edges on the cut block all paths from the source to the terminal, and thus the total flow cannot exceed their cumulative capacity. As one of the earliest and the fundamental results in combinatorial algorithms, Ford and Fulkerson proved that the capacity of a minimum cut is equal to the value of a maximum flow. This duality between maximum flow and minimum cut underlies many algorithms for flow problems, and in this work we compute the value of a maximum flow by finding the capacity of a minimum cut. A more detailed discussion on flow algorithms along with proofs of this duality can be found in [7, 30].

An example for the maximum flow minimum cut property is illustrated in Figure 6.1. In this figure, the numbers on the edges represent the flow assignment and the capacity of the edge. For instance, the edge from v_1 to v_3 has a capacity of 9 units and uses 7 units of this capacity in the current flow assignment. The volume of a maximum flow in this graph is 13 units, and the current flow assignment is optimal.

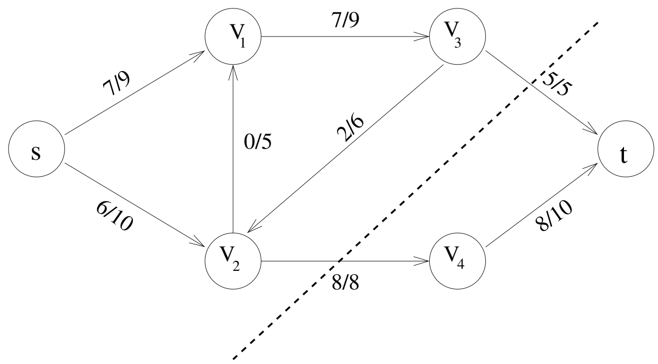

FIG. 6.1. *Maximum flow and minimum cut on a flow graph. Numbers on the edges represent flow assignment/capacity. The dashed line represents the cut.*

The associated minimum cut in this graph is $V_1 = \{s, v_1, v_2, v_3\}$ and $V_2 = \{v_4, t\}$ with capacity 13.

6.2. Network inhibition problem. In [24], Phillips defines the network inhibition problem as follows. Each edge in the network has a destruction cost, and a fixed budget is given to attack the network. A feasible attack removes a subset of the edges, whose total destruction cost is no greater than the budget, and the network inhibition problem is to find an attack that optimally reduces the value of a maximum flow in the graph after the attack. The network inhibition problem has two objectives and/or constraints: the cost of an attack and the resulting damage. Phillips's formulation, which we call the *maximum damage* version of the network inhibition problem, constrains the budget of the attack and seeks to maximize the damage. Here, we work on the *minimum cost* version of the problem, where we look for the most cost-effective attack, where the damage is no smaller that a specified bound.

The network inhibition problem is closely related to the maximum flow/minimum cut problem. More specifically, the minimum cut problem is a special version of the network inhibition problem, where the value of a maximum flow in the network after the attack should be zero. In terms of complexity, however, the network inhibition problem is much harder. While maximum flow problems can be efficiently solved by polynomial-time algorithms [15], the network inhibition problem is NP-complete [24]. Phillips provides a comprehensive study on the network inhibition problem [24]. Royset and Wood [27] studied this problem as a bi-objective problem, and Pinar, Fogel, and Lesieutre [25] studied the inhibiting bisection problem, where a graph decomposition with maximum production/demand mismatch is sought.

6.3. MILP formulation for the network inhibition problem. A formulation for the network inhibition problem requires measuring the value of a maximum flow on the graph after the attack, which we do by finding a minimum cut. For clarity of presentation, we first present an integer programming formulation of the minimum cut problem and then extend this formulation for the network inhibition problem.

6.3.1. MILP formulation for the minimum cut problem. Let $G = (V, E)$ be a flow network with n vertices and m edges, and let A be the $m \times n$ node-arc incidence matrix of this graph. We assume the first and last columns of A correspond to the source and terminal vertices, respectively. We use c_i to refer to the capacity of the ith line. We define a binary variable ρ_i for each vertex $v_i \in V$, so that

$$\rho_i = \begin{cases} 0, & \text{if } v_i \in V_1, \\ 1, & \text{if } v_i \in V_2, \end{cases}$$

where V_1 and $V_1 = V \setminus V_2$ denote the partitioning of V that defines the cut. We also define a binary variable ω_i for each edge, so that

$$\omega_i = \begin{cases} 1, & \text{if } e_i \text{ is on the cut}, \\ 0, & \text{otherwise}. \end{cases}$$

The minimum cut problem can then be formulated as follows:

$$\min_{\rho,\omega} \quad c^T \omega, \tag{6.1}$$

$$\text{s.t.} \quad A\rho - \omega \leq 0, \tag{6.2}$$

$$A\rho + \omega \geq 0, \tag{6.3}$$

$$\rho_1 = 0, \tag{6.4}$$

$$\rho_n = 1; \tag{6.5}$$

$$\rho_i \in \{0, 1\} \quad \text{for } i = 1, 2, \dots, n, \tag{6.6}$$

$$\omega_i \in \{0, 1\} \quad \text{for } i = 1, 2, \dots, m. \tag{6.7}$$

Here, the objective function minimizes the cumulative capacity of the cut edges. Constraints (6.4) and (6.5) guarantee that $s \in V_1$ and $t \in V_2$, respectively. Constraints (6.6) and (6.7) guarantee that the ρ and ω are binary variables. Constraints (6.2) and (6.3) are used to enforce any edge between parts V_1 and V_2 to be labeled as a cut edge. Consider an edge e_k that goes from v_i to v_j, for which we have the following constraints:

$$\rho_j - \rho_i - \omega_k \leq 0, \tag{6.8}$$

$$\rho_j - \rho_i + \omega_k \geq 0. \tag{6.9}$$

We need to show that $\omega_k = 1$, if v_i and v_j are on different parts ($\rho_i \neq \rho_j$). If $\rho_j = 1$ and $\rho_i = 0$, (6.8) forces ω_k to be $\geq$1. Symmetrically, if $\rho_j = 0$ and $\rho_i = 1$, it will be (6.9) that forces ω_k to be $\geq$1. When the two vertices are in the same part, i.e., $\rho_i = \rho_j$, ω_k can be either zero or one. However, since the objective is to minimize $c^T\omega$, when the edge is not on the cut, ω_k will be at its minimum, zero. This analysis further shows that we do not need to impose ω variables to be binary explicitly. When edge e_k is on the cut, we need $\omega_k \geq 1$, and when e_k is an internal edge, ω_k will be at its minimum due to the objective function. In an optimal solution to (6.1)–(6.6), ω variables naturally take binary values, when they are constrained to be in the $[0, 1]$ region. Therefore we can replace (6.7) with

$$0 \leq \omega_i \leq 1 \quad \text{for } i = 1, 2, \dots, m.$$

6.3.2. MILP formulation for the network inhibition problem. Since the network inhibition problem seeks to minimize the maximum flow/minimum cut of a graph in a cost optimal way, we can use our formulation for the minimum cut as the core of our formulation for the network inhibition problem. We start by defining a binary variable d_i for each edge that defines whether a line is destroyed.

$$d_i = \begin{cases} 1, & \text{if } e_i \text{ is destroyed}, \\ 0, & \text{otherwise}. \end{cases}$$

Let p be a vector that indicates line-destruction costs. The minimum cost version of the network inhibition problem can be formulated as a MILP problem as follows.

$$\min_{\rho,\omega} \quad p^T d, \tag{6.10}$$
$$\text{s.t.} \quad c^T \omega \leq S', \tag{6.11}$$
$$A\rho - (\omega + d) \leq 0, \tag{6.12}$$
$$A\rho + (\omega + d) \geq 0, \tag{6.13}$$
$$\rho_1 = 0, \tag{6.14}$$
$$\rho_n = 1; \tag{6.15}$$
$$\rho_i \in \{0, 1\} \quad \text{for } i = 1, 2, \ldots, n, \tag{6.16}$$
$$d_i \in \{0, 1\} \quad \text{for } i = 1, 2, \ldots, m, \tag{6.17}$$
$$\omega_i \in [0, 1] \quad \text{for } i = 1, 2, \ldots, m. \tag{6.18}$$

Here, the objective corresponds to minimizing the cost of the attack, and the ω vector identifies the cut edges on the remaining graph. While this cut is not necessarily the minimum cut, it provides an upper bound on the maximum flow in the graph, which is sufficient for our purposes. Inequality (6.11) guarantees the capacity of this cut, and thus the volume of a maximum flow is no bigger than a specified threshold S'. Equations (6.12)–(6.15) ensure that the ω vector identifies the cut edges. The source and the terminal vertices are on different parts of the cut due to (6.14) and (6.15), and for each line $e_k = (v_i, v_j)$ in the graph we have the following two constraints:

$$\rho_j - \rho_i - \omega_k - d_k \leq 0, \tag{6.19}$$
$$\rho_j - \rho_i + \omega_k + d_k \geq 0. \tag{6.20}$$

It suffices to show that $\omega_k = 1$, if v_i and v_j are on different parts ($\rho_i \neq \rho_j$) and the edge is not destroyed ($d_k = 0$). Note that we do not need to show that $\omega_k = 0$ for other cases, since $\omega_k > 0$ redundantly increases the $c^T\omega$ value, which we are trying to keep small. In other words, the ω vector defines a valid cut in the graph, but it is not necessarily minimum, and a subset of the edges it provides might provide a valid cut. If $\rho_j = 0$, $\rho_i = 1$, and $d_i = 0$, (6.19) forces $\omega_k \geq 1$. Symmetrically, if $\rho_j = 1$, $\rho_i = 0$, and $d_i = 0$, then it will be (6.20) that forces ω_k to be ≥ 1. Also observe that when $d_i = 1$, the two inequalities will be satisfied, regardless of ρ_i, ρ_j, and ω_k.

The formulation in (6.10)–(6.18) is the minimum cost version of the network inhibition problem, where we look for the most cost-efficient way to cause a damage of specified severity. We can easily switch the positions of the objective function and the severity constraint (6.11) for the maximum damage version of the problem, where we try to find an attack of specified cost that will give the maximum damage.

6.4. Power grid vulnerability as a network inhibition problem. The combinatorial version of the vulnerability analysis problem of section 5.2 can be posed as the network inhibition problem. Observe that the severity constraint, which we stated as the volume of load shed being above a threshold, S, can be rephrased as the remaining flow in the graph being below $S' = |G| - S$, where $|G|$ denotes the total generation in the system. Here, we replace the severity threshold S of the power grid vulnerability analysis with $|G| - S$ for the network inhibition problem. The graph of a power grid can be transformed to a flow graph by adding a source vertex s and a terminal vertex t, and connecting each generator to the source with an edge whose capacity is equal to the generation at that node and connecting each load to the terminal with an edge whose capacity is equal to the consumption at that node. All other edges that correspond to power lines retain their capacities by assigning the capacity of an edge as the capacity of the corresponding power line. We define the destruction cost of the source and terminal edges to be ∞, and all other edges to be 1, to guarantee that the solution to the network inhibition chooses only actual power lines to cut.

A solution to the network inhibition problem identifies a bipartitioning of the nodes into V_1 and V_2, which correspond to generation-rich region P_1 and load-rich region P_2, respectively. The cut edges potentially include source edges that connect s to generation nodes, terminal edges that connect t to terminal nodes, as well as edges that represent power lines. Observe that a source edge will be cut, if the respective generator is in V_2, and similarly a terminal edge will be cut if the respective load is in V_1. The capacity of the cut can then be expressed as $L(P_1) + G(P_2) + Cap(Lines(P1, P_2) \setminus C)$. Here $L(P_1)$ represents the total load in V_1 and is equal to the cumulative capacity of the terminal edges on the cut. Similarly, $G(P_2)$ represents the total generation in V_2 and is equal to cumulative capacity source edges on the cut. C is the set of cut edges identified by the d vector, and $Cap(Lines(P1, P_2) \setminus C)$ is the total capacity of the active edges on the cut that represent power lines. Constraint (6.11) then becomes

$$\begin{aligned}
L(P_1) + G(P_2) + Cap(Lines(P_1, P_2) \setminus C) &\leq |G| - S, \\
L(P_1) + |G| - G(P_1) + Cap(Lines(P_1, P_2) \setminus C) &\leq |G| - S, \\
L(P_1) - G(P_1) + Cap(Lines(P_1, P_2) \setminus C) &\leq -S, \\
-L(P_1) + G(P_1) - Cap(Lines(P_1, P_2) \setminus C) &\geq S,
\end{aligned}$$

which is the same as (5.11).

6.5. Solving the network inhibition problem. We applied our integer programming formulation for the network inhibition problem to identify vulnerabilities of a simplified model of the Western states power grid with 13,374 nodes and 16,520 lines. We used PICO [13], a massively parallel integer programming solver, developed at Sandia National Laboratories, to solve the associated MILP problems.

We solved instances of the network inhibition problem for the Western states power grid with varying number of lines being broken. The solution times for these problems were only in the order of tens of seconds on an Opteron 2.2 GHz processor with 4.4 GFlops/sec theoretical peak and 6 Gbytes of physical memory. These results show that our integer programming formulations are practical and are applicable to large systems.

7. Conclusions and future work. One of the most important criteria for the secure operation of the electric power grid is the identification of small groups of lines, the removal of which would cause a severe blackout. We first presented a bilevel mixed integer nonlinear programming (MINLP) formulation of this problem, and then described the associated optimality conditions. Our analysis of this formulation revealed a special combinatorial structure that we exploited to avoid nonlinearity and approximated the original problem as a pure combinatorial problem. The key new observation behind our analysis was the correspondence between the Jacobian matrix (a representation of the feasibility boundary of the power flow equations that describe the flow of power in the network) and the Laplacian matrix in spectral graph theory (a representation of the graph of the electric power grid). Our reduction allowed us to directly seek values of discrete variables in an optimal solution to our MINLP formulation, without explicitly solving the nonlinear part, thereby simplifying the problem complexity, both theoretically and practically. The reduced combinatorial problem is known as the network inhibition problem, for which we presented a mixed integer linear programming formulation. Our empirical studies demonstrated that our combinatorial approximation is accurate and efficient, especially as the blackout size increases, and we can solve the corresponding integer programming problems for problems with tens of thousands of lines.

This work leads to new research problems both for optimization and for power systems communities. First, we used a simplified model of power flow equations, where we fixed the voltages and focused only on active power. Our formulation can be easily extended to include reactive power, but our analysis of an optimal solution needs to be revised. It remains to be seen whether there exists a combinatorial structure when the reactive power is also included in the analysis. Another interesting question is whether it is possible to find tighter bounds for the flow between generation-rich and load-rich regions, as defined in section 5. We believe our current bound of cumulative sum of capacities of active lines can be improved by careful analysis of power flow equations, which will be an interesting question, especially for power systems experts. Finally, it would be interesting to include system dynamics in vulnerability analysis, without solving differential algebraic equations, where stochastic models might be useful.

On the optimization front, solving the bilevel MINLP formulation remains a challenge. In particular, using our discrete approximation within a decomposition method needs further investigation. Recall that our approximation involves more than merely solving for binary variables, where continuous variables for the nonlinear part are fixed. The reduced problem can foresee changes in the nonlinear part and directly seeks values of binary variables (i.e., the broken lines in this problem) in an optimal solution. Therefore, our reduction can still be used to accelerate a decomposition algorithm. We believe that these studies will be closely related to how flow between two regions can be bounded. Another area for further investigation is the development of improved solution methods for the network inhibition problem, and in particular the use of additional constraints that better bound the flow between two regions. Both heuristics and exact algorithms would be interesting in this context.

Finally, this article focuses on the formulations of the power grid vulnerability analysis problem. A more practical study that applies existing software tools and algorithms to our formulations will be valuable to identify new research directions.

REFERENCES

[1] *Power system test case archive*, available at http://www.ee.washington.edu/research/pstca/.

[2] F. Alvarado, I. Dobson, and Y. Hu, *Computation of closest bifurcations in power systems*, IEEE Trans. Power Syst., 9 (1994), pp. 918–928.

[3] D. Bienstock and S. Mattia, *Using mixed-integer programming to solve power grid blackout problems*, Technical report TR-2005-07, IEOR Department, Columbia University, New York, 2005.

[4] B. Carreras, V. Lynch, I. Dobson, and D. Newman, *Dynamics, criticality, and self-organization in a model for blackouts in power transmission systems*, in Proceedings of the 35th Hawaii International Conference on System Sciences, Hawaii, 2002.

[5] B. Carreras, V. Lynch, I. Dobson, and D. Newman, *Dynamical and probabilistic approaches to the study of blackout vulnerability of the power transmission grid*, in Proceedings of the 37th Hawaii International Conference on System Sciences, Hawaii, 2004.

[6] B. Carreras, V. Lynch, M. Sactjen, I. Dobson, and D. Newman, *Modeling blackout dynamics in power transmission networks with simple structure*, in Proceedings of the 34th Hawaii International Conference on System Sciences, Maui, Hawaii, 2001.

[7] T. Cormen, C. E. Leiserson, R. L. Rivest, and C. Stein, *Introduction to Algorithms*, The MIT Press, Cambridge, MA, 2001.

[8] I. Dobson, B. Carreras, V. Lynch, and D. Newman, *An initial model for complex dynamics in electric power system blackouts*, in Proceedings of the 34th Hawaii International Conference on System Sciences, Maui, Hawaii, 2001.

[9] I. Dobson, J. Chen, J. Thorp, B. Carreras, and D. Newman, *Examining criticality of blackouts in power system models with cascading events*, in Proceedings of the 35th Hawaii International Conference on System Sciences, Hawaii, 2002.

[10] I. Dobson, K. Wierzbicki, B. Carreras, V. Lynch, and D. Newman, *An estimator of propagation of cascading failure*, in Proceedings of the 39th Hawaii International Conference on System Sciences, Hawaii, 2006.

[11] V. Donde, V. Lopez, B. Lesieutre, A. Pinar, C. Yang, and J. Meza, *Identification of severe multiple contingencies in electric power networks*, in Proceedings of the 37th North American Power Symposium, Ames, IA, 2005.

[12] V. Donde, V. Lopez, B. Lesieutre, A. Pinar, C. Yang, and J. Meza, *Identification of severe multiple contingencies in electric power systems*, IEEE Trans. Power Syst., 23 (2008), pp. 406–417.

[13] J. Eckstein, W. Hart, and C. A. Phillips, *An object-oriented framework for parallel branch and bound: Inherently parallel algorithms in feasibility and optimization and their applications*, in Elsevier Scientific Series on Studies in Computational Mathematics, Elsevier, New York, 2001, pp. 219–265.

[14] M. Fiedler, *Algebraic connectivity of graphs*, Czech. Math. J., 23 (1973), pp. 298–305.

[15] A. V. Goldberg and S. Rao, *Beyond the flow decomposition barrier*, J. ACM, 45 (1998), pp. 783–797.

[16] J. Grainger and W. Stevenson, *Power System Analysis*, McGraw-Hill, New York, 1994.

[17] S. Grijalva and P. Sauer, *Static collapse and topological cuts*, in Proceedings of the 38th Hawaii International Conference on System Sciences, Hawaii, 2005.

[18] S. Grjialva and P. Sauer, *A necessary condition of power Jacobian singularity based on branch complex flows*, IEEE Trans. Circuits Systems-I: Regular Papers, 52 (2005), pp. 1406–1413.

[19] T. He, S. Kolluri, S. Mandal, F. Galvan, and P. Rastgoufard, *Identification of weak locations in bulk transmission systems using voltage stability margin index*, in Applied Mathematics for Restructured Power Systems: Optimization, Control, and Computational Intelligence, Springer, New York, 2005.

[20] J. Arroyo and F. Galiana, *On the solution of the bilevel programming formulation to the terrorist threat problem*, IEEE Trans. Power Syst., 20 (2005), pp. 789–797.

[21] B. Lesieutre, A. Pinar, and S. Roy, *Power system extreme event detection: The vulnerability frontier*, in Proceedings of the 41st Hawaii International Conference on System Sciences, Hawaii, 2008.

[22] B. Lesieutre, S. Roy, V. Donde, and A. Pinar, *Power system extreme event screening using graph partitioning*, in Proceedings of the 38th North American Power Symposium, Carbondale, IL, 2006.

[23] G. Oliviera, S. Binato, L. Bahiense, L. Thome, and M. Pereira, *Security-constrained transmission planning: A mixed-integer disjunctive approach*, in Optimization Online, 2004.

[24] C. A. Phillips, *The network inhibition problem*, in STOC '93: Proceedings of the twenty-fifth annual ACM symposium on Theory of Computing, ACM Press, New York, 1993, pp. 776–785.

[25] A. Pinar, Y. Fogel, and B. Lesieutre, *The inhibiting bisection problem*, Technical report LBNL-62142, Lawrence Berkeley National Laboratory, Berkeley, CA, 2006.

[26] A. Pinar, A. Reichert, and B. C. Lesieutre, *Computing criticality of lines in power systems*, in IEEE International Symposium on Circuits and Systems (ISCAS 2007), New Orleans, LA, 2007, pp. 65–68.

[27] J. Royset and R. Wood, *Solving the bi-objective maximum-flow network-interdiction problem*, INFORMS J. Comput., 19 (2007), pp. 175–184.

[28] J. Salmeron, K. Wood, and R. Baldick, *Analysis of electric grid security under terrorist threat*, IEEE Trans. Power Syst., 19 (2004), pp. 905–912.

[29] E. Scholtz, *Observer-based monitors and distributed wave controllers for electromechanical disturbances in power systems*, Ph.D. thesis, MIT, Cambridge, MA, 2004.

[30] R. E. Tarjan, *Data Structures and Network Algorithms*, SIAM Press, Philadelphia, 1998.